2023 45th Annual International Conference of the IEEE Engineering in Medicine & Biology Society (EMBC) | 979-8-3503-2447-1/23/$31.00 ©2023 IEEE | DOI: 10.1109/EMBC40787.2023.10340798

Cardiovascular response to closed-loop intraneural stimulation of the right vagus nerve: a proof-of-concept study*

C. Zinno, *Student Member, IEEE,* F. Agnesi, F. Bernini, K. Gabisonia, D. Terlizzi, F. A. Recchia, V. Lionetti, S. Micera, *Senior Member, IEEE*

***Abstract*—Vagus nerve stimulation (VNS) is an FDA-approved technique for the neuromodulation of the autonomic nervous system. There are many therapeutic applications where VNS could be used as a therapy, such as cardiovascular diseases, epilepsy, depression, and inflammatory conditions. Cardiovascular applications are particularly relevant, since cardiovascular diseases are the top causes of death worldwide. VNS clinical trials have been performed in the last 15 years for the treatment of heart failure (HF), achieving controversial results. Typically VNS is applied with a cuff electrode placed around the nerve, in an open-loop or cardiac synchronized design. The effectiveness of this approach is hindered by the multifunctional nature of the VN, which is involved in a variety of homeostatic controls. When a high current is applied, adverse effects arise from the stimulation of undesired fibers. An alternative strategy is represented by intraneural stimulation, which can guarantee higher selectivity. Moreover, closed-loop modalities allow the delivery of electrical current inside the nerves only if needed, with a reduced risk of untargeted nerve activation and lower energy consumption. Here we propose a closed-loop intraneural stimulation of the right cervical VN in a clinically relevant animal model. The intraneural was designed according to the internal structure of the VN. A threshold-based closed-loop algorithm was developed using HR as a control variable to produce a chronotropic effect.**

***Clinical Relevance*—This work analyzes the closed-loop intraneural VNS for the treatment of cardiovascular disorders, and supports the possibility of developing fully implantable devices with a high degree of selectivity in stimulation and prolonged lifespan.**

I. Introduction

The vagus nerve (VN) is the main component of the parasympathetic nervous system, responsible for many homeostatic functions (e.g heart rate control, respiration, digestion) [1] thanks to its multifascicled structure [2]. The electrical modulation of VN activity can be exploited for the prevention and treatment of the disorders of vital organs. The Vagus Nerve Stimulation (VNS) consists of the activation of the VN fibers to modulate physiological functions. So far, it is an FDA-approved therapy for epilepsy, depression, stroke, and is currently under study for the treatment of cardiovascular diseases [3]–[7], which represent a major cause of morbidity and mortality worldwide [8]. The vagal innervation of the heart plays a critical role in the modulation of the heart rate that may affect myocardial perfusion. In particular, the right vagus nerve has stronger effect on heart rate [9]. Three main clinical trials have been performed for the treatment of heart failure (HF) by cervical vagal nerve stimulation using cuff electrodes in both open-loop (NECTAR-HF [3] and ANTHEM-HF [10] trials) and heartbeat-synchronized settings (INOVATE-HF trial [11]),. Unfortunately, this modality of VNS does not always exert a favorable hemodynamic effect associated with a better prognosis in patients with heart failure. Some limitations of these studies could be related to insufficient energy delivered and the lack of selectivity in extraneural stimulation, which could produce adverse effects (i.e neck contractions, cough, hoarseness). New technologies to optimize patient care by cardiac VNS are expected. First, electrodes can be implanted inside the nerve in close contact with the internal fascicles, allowing for better selectivity of stimulation while reducing the amount of current delivered. Second, closed-loop stimulation protocols can be used to prolong the lifespan of implantable devices by delivering the appropriate amount of current to the VN only as needed, thus reducing power consumption. To date, many closed-loop VNS strategies using cuff electrodes have been implemented for cardiovascular applications [12]–[14]. However, none of them involved the use of intraneural electrodes.

Here we propose a closed-loop VNS system exploiting the properties of intraneural stimulation. A domestic pig was used as human-relevant large animal model to test safety and evaluate hemodynamic effects of our device.

II. Material and Methods

A. Electrode design and fabrication

A custom intraneural thin film polyimide electrode was used to perform VN stimulation, inspired by the TIME design [15]. The dimensions of the electrode and the distribution of the active sites (16 circular active sites, 80 µm diameter, Au with

*Research supported by H2020-FETPROACT-2018-2020 NEUHEART Project #824071. C.Z, F.A are with The BioRobotics Institute, Department of Excellence in Robotics & AI, Scuola Superiore Sant'Anna, Pisa, Italy (corresponding author to provide phone: +393311601948; e-mail: ciro.zinno@santannapisa.it). F. B., K.G are with BioMedLab, Scuola Superiore Sant'Anna, Pisa, Italy. D.T is with Fondazione Toscana G. Monasterio, Pisa, Italy. F. A. R is with the Scuola Superiore Sant'Anna, Pisa, Italy, National Research Council, Pisa, Italy; Cardiovascular Research Center, Lewis Katz School of Medicine at Temple University, Philadelphia, PA, United States of America. V.L is with Unit of Translational Critical Care Medicine, Laboratory of Basic and Applied Medical Sciences, Interdisciplinary Research Center "Health Science", and BioMedLab, Scuola Superiore Sant'Anna, Pisa, Italy, and S.M is with The BioRobotics Institute, Department of Excellence in Robotics & AI, Scuola Superiore Sant'Anna, Pisa, Italy; Bertarelli Foundation Chair in Translational NeuroEngineering, Centre for Neuroprosthetics and Institute of Bioengineering, École Polytechnique Fédérale de Lausanne (EPFL), Lausanne, Switzerland.

IrOx coating) were designed according to histological analysis [16]. The fabrication process was performed according to standard microfabrication techniques [15]–[17]. Briefly, a 5 µm-thick layer of polyimide (PI2611, HD Microsystems GmbH) was spin-coated on a silicon wafer, then a thermal curing process was executed. A first photolithographic step was performed, including spin-coating, baking, exposing, and developing a 4 µm-thick photoresist (ECI 3027). Then, a conductive layer of Ti/Pt/IrOx (25/300/400 nm) was sputtered (AC450, Alliance Concept) and patterned thanks to lift-off. Spin-coating and curing processes were repeated for a second layer of polyimide, 5 µm-thick to isolate and encapsulate the conductive tracks. A second photolithographic step (AZ10XT 12 µm) was performed, followed by O2-based reactive ion etching (RIE). The RIE was used to obtain the desired shape of the device and expose the active sites and the electrical connections. The devices were then released through an anodic dissolution of aluminum in a 1.5 V bias in a saturated NaCl solution. The electrode was then connected to custom flexible PCBs through Ag and biocompatible UV glue; similarly to the TIME design, it was folded to insert a suture thread inside to perform the implantation.

B. Surgical preparation

All animal procedures were approved by the Italian Ministry of Health (no. 76/2014 PR) and conducted in conformity with the guidelines from Legislative Decree n°26/2014 of Italian Ministry of Health, Directive 2010/63/EU of the European Parliament, and the guidelines for the Care and Use of Laboratory Animals (NIH publication No. 85–23).

One healthy male sexually mature domestic pig (30 kg, body weight) was studied. The animal was pre-medicated using Zoletil® (10 mg/kg) and Stressnil® (1 mg/kg). Then, it was anesthetized using Propofol (2 mg/kg intravenously) and maintained under 1-2 % sevoflurane in air enriched by 50 % oxygen during mechanical ventilation [18], [19]. To expose the cervical region of the right VN, an anterior longitudinal neck incision was performed and the VN was isolated away from the carotid artery and the surrounding connective sheath tissue. The intraneural electrode was inserted transversally into the cervical region of the VN (Figure 1), and connected to a portable stimulator [20].

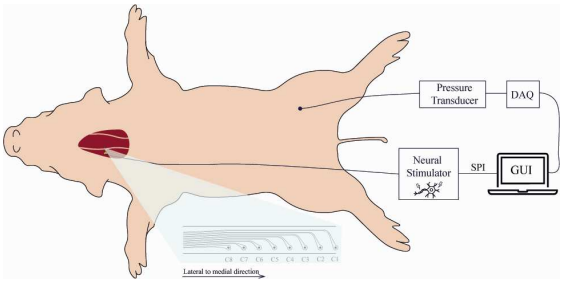

Figure 1: Experimental setup. The intraneural electrode is implanted in the right cervical VN and connected to a portable stimulator. The current is delivered through the stimulator, controlled by a GUI. The blood pressure is measured with a pressure transducer at the level of the femoral artery and recorded with a DAQ connected to a host PC.

C. Closed-loop algorithm

A threshold-based algorithm for the closed-loop stimulation was developed in LabView 2021 SP1 (National Instrument, USA), and deployed on a host PC, using the heart rate (HR) as a control variable (Figure 2). The arterial blood pressure (BP) signal was measured via a fluid filled catheter inserted trough the femoral artery, attached to a P23ID strain-gauge transducer and sampled with a data acquisition board (DAQ, National Instrument, USA) at 40 Hz. The BP signal was used to compute the instantaneous HR. First, the BP signal was low-pass filtered with a cutoff frequency of 5 Hz. Then, to guarantee a more precise and reliable calculation, the slope sum function (SSF) was used to enhance the slopes of the BP signal (1), to properly detect the systolic peaks and compute the HR [21]

$$z_i = \sum_{k=i-w}^{i} \Delta u_k, \qquad \Delta u_k = \begin{cases} \Delta y_k : \Delta y_k > 0 \\ 0 : \Delta y_k < 0 \end{cases} \qquad (1)$$

where w is the analyzing window, $\Delta y_k = y_k - y_{k-1}$, and y_k is the low-pass filtered BP signal. To obtain the maximal efficacy for the SSF, w was set to a value that approximates the upslope phase of the BP signal (~ 128 ms), thus for a 40 Hz sampling rate it was set to 7 samples. HR was calculated as the inverse of time interval between two successive systolic peaks. Once the HR was computed, the 60 last values were stored in a circular buffer and the HR signal was filtered with an exponential moving average (EMA) filter (α = 0.15, forgetting factor). The EMA filtering was performed to give more relevance to the most recent values of the HR. Then, stimulation was delivered only when the filtered HR value exceeded a predefined threshold (the desired HR value).

D. Experimental protocol

Following baseline measurements, the current was injected through a single active site of the electrode. The active site giving the highest physiological response was identified in advance in an open-loop setting where all the contacts were tested with the same current parameters. VNS was delivered as a cathodic-first, charge-balanced, biphasic rectangular wave with an amplitude of 500 µA, a frequency of 10 Hz, and a pulse width of 200 µs. An HR value was first imposed for 3 minutes to trigger the stimulation, after which a new HR threshold was imposed each 3 minutes. For the offline analysis, systolic and diastolic arterial BP were recorded for each heartbeat and low-pass filtered with a cutoff frequency of 5 Hz to remove artifacts related to the breathing rhythm.

III. Results

A. Physiological responses to closed-loop VNS

The active site C7 (Figure 1) was identified as the one yielding the highest response in the open loop sessions,

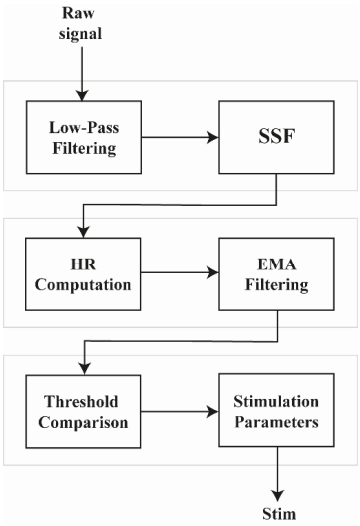

Figure 2: Block diagram of the closed-loop algorithm. The raw signal is low-pass filtered (LPF, cut-off signal 5 Hz) and then the SSF is computed. From the SSF the HR can be retrieved as the distance between the peaks divided by the time interval between them. The HR is EMA filtered ($\alpha = 0.15$) to give more relevance to the most recent samples. The stimulation starts when the filtered HR overcomes a threshold, with pre-defined parameters.

therefore it was selected for the VNS in the closed-loop session. HR, diastolic and systolic BP responses to closed-loop VNS are shown in Figure 3. No contraction of muscles or signs of arrhythmia were observed during VNS. HR results are presented after moving average filtering (n=30 samples, Figure 3, top). When the HR threshold was set to 55 BPM, the HR rapidly started to decrease from the baseline condition. Nevertheless, the HR reached a plateau at 56.5 BPM, which was kept for the entire duration of the stimulation (3 minutes). When the HR threshold was changed to 58 BPM, the HR increased and then stabilized to the threshold value. The same response was observed at higher HR threshold value (59.5 BPM). Diastolic (Figure 3, middle) and systolic (Figure 3, bottom) BP changed in line with HR response. Specifically, VNS induced a rapid reduction of BP that progressively increased after a few second without reaching baseline values. As the HR threshold increased, we observed a rapid elevation in BP values followed by a subsequent decrease, consistent with the reduction in HR.

IV. Discussions

A. Physiological responses to closed-loop VNS

The preliminary results of our proof-of-concept study show that the closed-loop intraneural VNS can finely modulate the heart rate and the rate-dependent systemic blood pressure. The time dynamics of the HR changes at different threshold tends to be slow, as shown in Figure 3 , although it is strongly influenced by the MA filtering used to show the data. Our data will support further analysis to confirm this effect even during changes of BP.

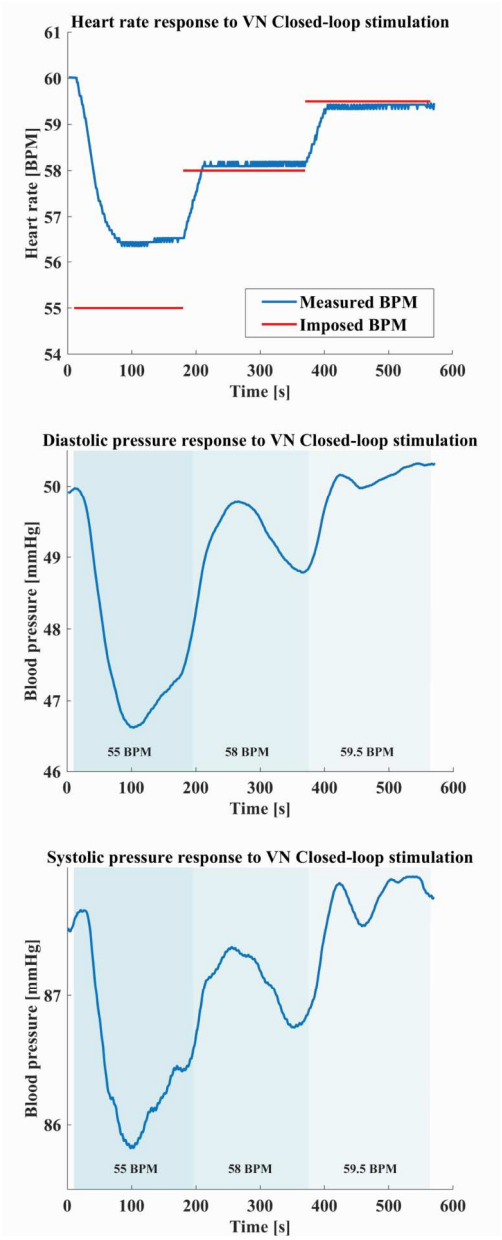

Figure 3: Physiological responses to closed-loop VNS. Top: HR response, middle: diastolic BP response, bottom: systolic BP response. The dark/ light/ very light blue shades in the diastolic and systolic BP plots represent the different HR thresholds imposed during a specific time interval, indicated by the corresponding values at the bottom of the plots. When VNS is applied, HR starts decreasing rapidly, followed by a slower decrease in diastolic and systolic BP. When the HR threshold is updated, the HR starts increasing and then stabilizes to the new updated value, while the diastolic and systolic BP dynamics is slower.

The right VNS by intraneural electrodes allows injecting current into the nerve without causing adverse effects, since the electrical field produced with the current applied (500 µA) is small and activates only a small number of fascicles. However, this could also have some drawbacks; stimulation might not be able to activate the target fascicles (i.e cardiac fascicles) when the electrode is not implanted in close enough proximity, thus not producing a physiological response. In

accordance, it is interesting to note as shown in Figure 3, top, that the HR never reached the value imposed from the first HR threshold. This can also lead to an imprecise conversion of the HR threshold in corresponding stimulation pulses needed, since the values could change according to electrode implantation location and anatomical variability. It is conceivable that the electrode leads to only partial recruitment of the target fibers. Indeed, the absolute value of the variations induced by our intraneural VNS is small. Conversely, other studies achieve better results with different electrodes. Blanz et. al [22] have observed HR reduction of 30-40 BPM following cervical VNS in pigs. However, the chronotropic response could not be elicited without inducing adverse effects, due to off-target stimulation of undesired fascicles. More accurate procedures of implantation for intraneural electrodes should be developed to achieve a similar HR chronotropic response with this kind of device.

B. Limitations of the study

Currently, all the systems (acquisition, processing, SPI with stimulator) run on a host PC, which expose to hardware limitations for the sampling rate of the raw signal. This also has an impact on the HR computation. In the next experiments, all the systems will be deployed to dedicated hardware, and the algorithm will be implemented in a real-time framework. Finally, future studies in awake animals using implantable sensors will improve real-time measurement of HR and BP response to VNS without the interference of anesthetics.

V. Conclusion

We developed and tested in an anesthetized domestic pig a new closed-loop system for intraneural stimulation of right VN, leading to fine modulation of heart rate-dependent hemodynamic response. This work paves the way to a fully implantable closed-loop VNS system that minimizes the adverse effects of untargeted electrical stimulation, while reducing energy consumption.

Acknowledgment

The authors would like to thank the European Commission for funding the H2020-FETPROACT-2018-2020 NEUHEART Project #824071 which made this work possible.

References

[1] H. Yuan and S. D. Silberstein, “Vagus Nerve and Vagus Nerve Stimulation, a Comprehensive Review: Part I,” *Headache: The Journal of Head and Face Pain*, vol. 56, no. 1, pp. 71–78, 2016, doi: 10.1111/head.12647.

[2] N. Jayaprakash *et al.*, “Organ- and function-specific anatomical organization and bioelectronic modulation of the vagus nerve.” bioRxiv, p. 2022.03.07.483266, Mar. 10, 2022. doi: 10.1101/2022.03.07.483266.

[3] G. M. De Ferrari *et al.*, “Long-term vagal stimulation for heart failure: Eighteen month results from the NEural Cardiac TherApy foR Heart Failure (NECTAR-HF) trial,” *International Journal of Cardiology*, vol. 244, pp. 229–234, Oct. 2017, doi: 10.1016/j.ijcard.2017.06.036.

[4] R. K. Premchand *et al.*, “Autonomic regulation therapy via left or right cervical vagus nerve stimulation in patients with chronic heart failure: results of the ANTHEM-HF trial,” *J Card Fail*, vol. 20, no. 11, pp. 808–816, Nov. 2014, doi: 10.1016/j.cardfail.2014.08.009.

[5] I. S. Anand *et al.*, “Comparison of symptomatic and functional responses to vagus nerve stimulation in ANTHEM-HF, INOVATE-HF, and NECTAR-HF,” *ESC Heart Failure*, vol. 7, no. 1, pp. 76–84, 2020, doi: 10.1002/ehf2.12592.

[6] D. T. T. Plachta *et al.*, “Blood pressure control with selective vagal nerve stimulation and minimal side effects,” *J. Neural Eng.*, vol. 11, no. 3, p. 036011, May 2014, doi: 10.1088/1741-2560/11/3/036011.

[7] M. Donegà *et al.*, “Human-relevant near-organ neuromodulation of the immune system via the splenic nerve,” *Proc Natl Acad Sci USA*, vol. 118, no. 20, p. e2025428118, May 2021, doi: 10.1073/pnas.2025428118.

[8] E. Wilkins *et al.*, *European Cardiovascular Disease Statistics 2017*. Brussels: European Heart Network, 2017.

[9] G. A. Ng, K. E. Brack, and J. H. Coote, “Effects of direct sympathetic and vagus nerve stimulation on the physiology of the whole heart--a novel model of isolated Langendorff perfused rabbit heart with intact dual autonomic innervation,” *Exp Physiol*, vol. 86, no. 3, pp. 319–329, May 2001, doi: 10.1113/eph8602146.

[10] K. Sharma *et al.*, “Long-term Follow-Up of Patients with Heart Failure and Reduced Ejection Fraction Receiving Autonomic Regulation Therapy in the ANTHEM-HF Pilot Study,” *International Journal of Cardiology*, vol. 323, pp. 175–178, Jan. 2021, doi: 10.1016/j.ijcard.2020.09.072.

[11] M. R. Gold *et al.*, “Vagus Nerve Stimulation for the Treatment of Heart Failure,” *Journal of the American College of Cardiology*, vol. 68, no. 2, pp. 149–158, Jul. 2016, doi: 10.1016/j.jacc.2016.03.525.

[12] H. M. Romero-Ugalde *et al.*, “A novel controller based on state-transition models for closed-loop vagus nerve stimulation: Application to heart rate regulation,” *PLOS ONE*, vol. 12, no. 10, p. e0186068, Oct. 2017, doi: 10.1371/journal.pone.0186068.

[13] D. T. T. Plachta, J. Zentner, D. Aguirre, O. Cota, T. Stieglitz, and M. Gierthmuehlen, “Effect of Cardiac-Cycle-Synchronized Selective Vagal Stimulation on Heart Rate and Blood Pressure in Rats,” *Adv Ther*, vol. 33, no. 7, pp. 1246–1261, Jul. 2016, doi: 10.1007/s12325-016-0348-z.

[14] Y. Zhou *et al.*, “An Implanted Closed-loop Chip System for Heart Rate Control: System Design and Effects in Conscious Rats,” *J Biomed Res*, vol. 24, no. 2, pp. 107–114, Mar. 2010, doi: 10.1016/S1674-8301(10)60018-8.

[15] T. Boretius *et al.*, “A transverse intrafascicular multichannel electrode (TIME) to interface with the peripheral nerve,” *Biosensors and Bioelectronics*, vol. 26, no. 1, pp. 62–69, Sep. 2010, doi: 10.1016/j.bios.2010.05.010.

[16] I. Strauss, C. Zinno, A. Giannotti, M. M. Ottaviani, F. A. Recchia, and S. Micera, “Adaptation and Optimization of an Intraneural Electrode to Interface with the Cervical Vagus Nerve,” in *2021 10th International IEEE/EMBS Conference on Neural Engineering (NER)*, May 2021, pp. 116–119. doi: 10.1109/NER49283.2021.9441131.

[17] A. Cutrone *et al.*, “A three-dimensional self-opening intraneural peripheral interface (SELINE),” *J. Neural Eng.*, vol. 12, no. 1, p. 016016, Jan. 2015, doi: 10.1088/1741-2560/12/1/016016.

[18] D. Ferraro *et al.*, “Implantable Fiber Bragg Grating Sensor for Continuous Heart Activity Monitoring: Ex-Vivo and In-Vivo Validation,” *IEEE Sensors Journal*, vol. 21, no. 13, pp. 14051–14059, Jul. 2021, doi: 10.1109/JSEN.2021.3056530.

[19] V. Lionetti *et al.*, “Impact of Acute Changes of Left Ventricular Contractility on the Transvalvular Impedance: Validation Study by Pressure-Volume Loop Analysis in Healthy Pigs,” *PLoS One*, vol. 8, no. 11, p. e80591, Nov. 2013, doi: 10.1371/journal.pone.0080591.

[20] Y. Wu, D. Jiang, and A. Demosthenous, “A Multi-Channel Stimulator With High-Resolution Time-to-Current Conversion for Vagal-Cardiac Neuromodulation,” *IEEE Transactions on Biomedical Circuits and Systems*, vol. 15, no. 6, pp. 1186–1195, Dec. 2021, doi: 10.1109/TBCAS.2021.3139996.

[21] W. Zong, T. Heldt, G. B. Moody, and R. G. Mark, “An open-source algorithm to detect onset of arterial blood pressure pulses,” in *Computers in Cardiology, 2003*, Sep. 2003, pp. 259–262. doi: 10.1109/CIC.2003.1291140.

[22] S. L. Blanz *et al.*, “Spatially selective stimulation of the pig vagus nerve to modulate target effect versus side effect.” bioRxiv, p. 2022.05.19.492726, May 20, 2022. doi: 10.1101/2022.05.19.492726.